Insights into ultrasound-promoted degradation of naphthenic acid compounds in oil sands process affected water. Part II: In silico quantum screening of hydroxyl radical initiated and propagated degradation of benzoic acid

Kirpalani, Deepak M.; Nong, Andy; Ansari, Rija

Publisher's version / Version de l'éditeur:
https://doi.org/10.1016/j.ultsonch.2022.105983
Ultrasonics Sonochemistry, 85, C, 2022-03-15

Ultrasonics Sonochemistry 85 (2022) 105983

Contents lists available at ScienceDirect

Ultrasonics Sonochemistry

journal homepage: www.elsevier.com/locate/ultson

Insights into ultrasound-promoted degradation of naphthenic acid compounds in oil sands process affected water. Part II: *In silico* quantum screening of hydroxyl radical initiated and propagated degradation of benzoic acid

Deepak M. Kirpalani *, Andy Nong, Rija Ansari

National Research Council of Canada, Energy Mining and Environment Portfolio, 1200 Montreal Road, Ottawa, ON K1A 0R6, Canada

ARTICLE INFO

Keywords:
Quantum mechanics
In silico screening
Benzoic acid
Naphthenic acids
Degradation modeling
Density functional theory

ABSTRACT

In Part I, we outlined the importance of sustainable sonochemical treatment to intensify oil sands process affected water (OSPW) treatment empirically and hypothesized degradation pathways. Herein, we elucidate the formation of intermediate products with well-defined molecular level solutions. Proposed mechanisms describe hydroxylation, decarboxylation and bond scission which drive the degradation of intermediates towards mineralization. This comprehensive first study on *in silico* screening of sonochemical degradation investigates quantum methods using density functional theory to explain the postulated degradation mechanisms through a theoretical radical attack approach, based on condensed Fukui reactivity indicators. A nudged elasticity band (NEB) approach is applied to find a minimum energy path (MEP), allowing the determination of intermediate products and energy barriers associated with naphthenic acid degradation. This approach provides structures and energies of the breakdown compounds formed along the reaction pathway enabling the determination of molecular reaction kinetics.

In continuation of Part 1, the focus of this study is to evaluate sonochemically-induced hydroxyl radical ($OH^{\bullet}$) reactions of benzoic acid using density functional theory. Hydroxylation and decarboxylation mechanisms of the model naphthenic acid compound and its intermediates were simulated to determine the prospective pathway to ideal mineralization. DFT was applied to calculate interaction energies, Mulliken charges, Hirshfeld population analysis, dipole moments, frontier orbitals, and polarizability. Electronic properties and frontier orbital trends were also compared to computational work by Riahi *et al.* [1] to confirm the transition states by Nudged Elastic Band Transition State theory (NEB-TS). In combination with Hirshfeld Population analysis, Fukui indices suggest a more linear degradation pathway narrowed down from earlier experimental work by Singla *et al.* [2]. The linear free energy relationship for the newly suggested computational benzoic acid degradation can be determined by $\ln(k_{TST/W}) = -1.677\Delta G - 15.41$ with a R^2 of 0.9997 according to classic transition state theory and Wigner tunneling. This computational method can be used to explore possible degradation pathways of other NAs and bridges molecular-to-macroscale sonochemical degradation of NA's through a manifestation of molecular solutions.

1. Introduction

Naphthenic acids (NAs) play a putative role as emerging contaminants in oil sands process affected water (OSPW), and remediation has become an increasing logistic and environmental concern. NAs are classified as a diverse and complex resin group of aliphatic and alicyclic naturally occurring carboxylic acids in crude oil. They are represented by the general formula of $C_nH_{2n-z}O_2$, (where n represents the number of carbon atoms and z represents the hydrogen deficiency) and consist of aromatic rings, unsaturated chains and heteroatoms of oxygen, sulfur, and nitrogen. During crude oil processing, naphthenic acids can partition into produced water due to changes in process temperature and pressure, pH and salinity. Water contamination by hazardous naphthenic acids has been a matter of international concern. A major thrust

* Corresponding author.
E-mail address: Deepak.Kirpalani@nrc-cnrc.gc.ca (D.M. Kirpalani).

https://doi.org/10.1016/j.ultsonch.2022.105983
Received 31 December 2021; Received in revised form 11 March 2022; Accepted 13 March 2022
Available online 15 March 2022

in oil sands upgrading and refining operations is towards the reuse of produced water to reduce fresh water intake. However, produced water recycling faces some significant challenges as it can lead to downstream corrosion, emulsion formation, deposition in processing units and acute toxicity on various aquatic organisms. Consequently, OSPW cannot be released into natural water sources and is stored in large tailing ponds until a comprehensive treatment process can be established. Although, toxicity of OSPW reduces, the concentration of naphthenic acids plateaus for decades due to its recalcitrant nature [3].

A continuous search for innovative technologies to address the treatment of produced water include advanced oxidative degradation of NA's is underway in the oil sands industry. Generally, such processes apply hybrid approaches such as ultraviolet irradiation with ozonation, hydrogen peroxide addition with sonochemical treatment or titania (TiO_2) nanoparticle-assisted photocatalytic degradation to maximize the oxidative destruction. The industrial process to remove NAs from crude oil in terms of upgrading the quality has improved over time with dilution, caustic washing, esterification, and catalytic decarboxylation [4]. Combination remediation efforts have room for improvement and additionally do not provide insight into individual process effects on degradation.

Ultrasound sonochemistry, has been applied extensively to degrade organic chemical pollutants within aqueous solutions. It was shown in Part I that ultrasound can breakdown NA compounds to lower toxicity and optimization of ultrasound processes can lead to mineralization of NA's to water and CO_2. Although, many sonochemical destruction studies of naphthenic acid compounds were reported, the absence of OSPW standards has led to multiple studies with various NA structures, concentrations and ultrasound conditions. Sonochemical effects; as by-products of acoustic waves, produced as mechanical oscillations propagating through an elastic (fluid) medium, are characterized into (1) Thermal decomposition or pyrolysis of the solvent, solute, vapor and gases present in the solution during the violent collapse conditions and (2) Radical chemistry that occurs in the cavity formed, at the bubble (cavity) interface and within the bulk medium.

Current literature highlights the selection of model naphthenic acids to extrapolate their degradation behaviours to the class as a whole. A thorough experimental study of the sonolytic degradation of benzoic acid [2] provides the basis for the degradation pathway in this 2-part study. Given a range of potential reactions along with the high variability in naphthenic acid compounds, this study attempts a validated *in silico* screening approach for determining sonochemical degradation pathways via $OH^{\bullet}$ and other oxidative products including further degradation of intermediate products. A radical attack approach, based on Fukui coefficients (reactive indicators), was applied to understand and devise a nudged elasticity band to determine reaction pathways for the products formed.

This study explores the QM screening strategy through the known degradation pathway of benzoic acid and its intermediates via a theoretical approach using DFT studies to complete mineralization from previous works and our previous study [5]. Geometry optimizations, frequency calculations, transitions states, interaction energies, Mulliken charges, Hirshfeld population analysis, dipole moments, and polarizabilities have all been calculated by DFT method.

1.1. Physical explanation of radical attack models

A number of reactive chemistry models have been proposed to explain sonochemical destruction in the vicinity of cavities generated during the process. Vapor-filled cavities from the solvent or volatile solute, present during collapse, undergo extreme conditions of temperature and pressure that lead to homolytic bond breakage to generate reactive radical or other species. The sonolysis of water produces $H^{\bullet}$ and $OH^{\bullet}$. The presence of O_2 vapor in the bubble is known to foster hydroxylation and decarboxylation reactions by formation of a peroxyl radical or undergoing thermolysis to produce an excited oxygen atom that further forms a hydroxyl radical species [6,7]. A reaction shift towards $OH^{\bullet}$ radicals may be enhanced by the introduction of ozone or similar oxidants into the process. It was reported and confirmed [5] that during sonication, model organic acids such as benzoic acid, due to their volatile and hydrophobic nature, diffuse to the cavitation bubble and decompose by pyrolysis and/or $OH^{\bullet}$ degradation by a range of steps as shown in Fig. 1.

1.2. Computational approach

Quantum computational methods play an important role in the determination of an energy profile that explains the formation of dissociation products. A density functional theory (DFT) approach is proposed in this study, to determine the degradation intermediates and products from benzoic acid, a model organic acid found in naphthenic acids.

Analysis of degradation of organic molecules using conventional DFT approaches can explain molecular radical chemistry and can provide fundamental insight into non-volatile sonochemical reactions. Energy profiles between a precursor and the product can be calculated using intrinsic reaction coordinates. However, the use of conventional intrinsic reaction coordinates requires a priori knowledge of the transition states of the quantum structures in the sonochemical degradation pathway. Hence, computational analysis of the energy profiles that occur in the vicinity of a sonochemical bubble during collapse remains a challenge. A minimum energy path (MEP) that connects the initial and final states with the highest statistical probability can be determined from the energy profile as the maximum volume of the minimum energy path occurs at the saddle points of its potential energy surface.

In this work, we propose the use of condensed Fukui indices to determine the reactive sites and a nudged elasticity band (NEB) approach that depends on the initial reactant and final decomposition products to determine the reaction pathway. Using the NEB approach, the energy profile of a fragmentation pathway supports the determination of the dissociation products that form during sonochemical reactions. NEB is an efficient approach for calculating the MEP between the initial and final states. A major benefit of this approach is the search of a saddle point considerably faster than conventional IRC method and at the same level as *ab initio* modeling. Herein, the NEB approach is applied to determine the sonochemical pathway of degradation of benzoic acid.

2. *In silico* screening method

QM calculations were performed with density functional theory (DFT) using Becke's thee-parameter hybrid functional [8] along with non-local correlation functional B3LYP [9,10]. The chemical structure of benzoic acid and intermediate carboxylic acids (e.g. muconic, maleic, fumaric, acetic, etc.) were prepared in the Avogadro program and initially optimized with MMFF94 force fields [11] using the software's auto optimization feature. Further geometrical optimizations, frequency, and Nudged Elastic Band Transition State (NEB-TS) computations were performed at the B3LYP/def2-svp level. Harmonic frequencies were determined to confirm products, reactants, and identified transition state correspond to energy minima. The reaction kinetics were determined using KiSThelP software developed for statistical mechanics studies from ab initio quantum chemistry data and do not require an expression for the potential energy term. The harmonic frequencies were applied to determine the ensuing reactions rate constants and thermodynamic properties using KiSThelP software. Interaction energies and other electronic properties such as dipole moments, polarizability, Mulliken charges, Hirshfeld population values, and energies of the frontier molecular orbital were also determined at the B3LYP/def2-svp level of theory. All quantum mechanical calculations were performed in the ORCA 4.2 software. The interaction energies were corrected for any basis set superposition errors using the counterpoise

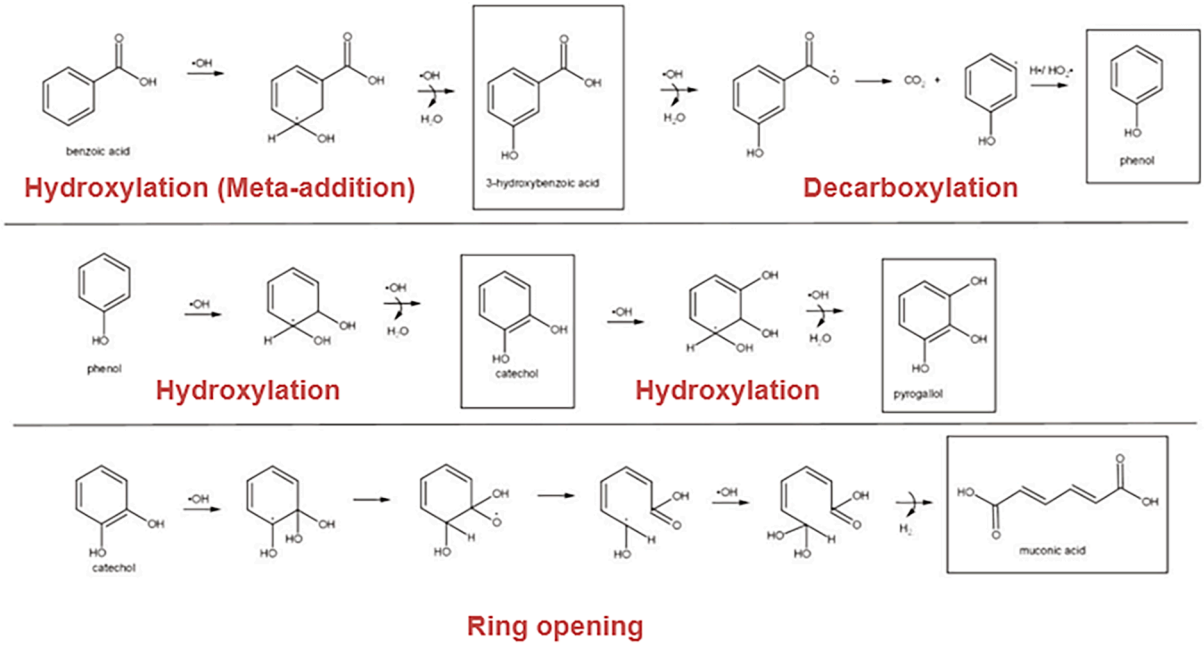

Fig. 1. Initial sonochemical degradation mechanism for BA through H-abstraction and decarboxylation reactions [2,5].

D4 method [12,13]) in ORCA.

The NEB-TS method, derived from nudged elastic band with transition state optimization, was used to find the transition state structure only from the geometries of the reactants and products. To extend the NEB-TS calculations, the self-consistent field convergence requirement was removed (noSCF) as it only eased NEB-TS convergence and did not affect the minimum energy pathway determination. The NEB-TS determined reactions were further validated with KiSThelP and Multiwfn program wherever applicable. Radicals were substituted with similar molecules such as an $OH^{\bullet}$ with a water molecule to keep the charge and spin state the same throughout a reaction step when needed. Ten NEB images were used to create a detailed reaction profile. Based on the empirical identification of degradation compounds from Part I [5], a suggested transition state was applied in ring-opening reaction steps to facilitate the reaction progress within NEB-TS and avoid radical attacks expected due to the limitations of the NEB-TS approach. Avogadro auto optimization was used to obtain the suggested transition states of the targeted reaction by selecting an arbitrary step immediately following radical attack.

The energy threshold for the climbing images using the NEB-TS model defaults to 2.00E-02 Eh/Bohr. Using the NEB method is dependent upon generating an initial guess for the images lying between the initial and final states. The image dependent pair potential (IDPP) is a novel approach to provide an improvement to the initial guess for the NEB path. The IDPP method applies the bond distance between the atoms involved in the transition state to create target structures for the images, rather than interpolating the atomic positions. By defining an objective function in terms of the distances between atoms, the NEB algorithm is used with this image dependent pair potential (IDPP) to create the initial guess for performing NEB calculations.

The IDPP default parameters used in the study include: convergence tolerance of 0.0100 1/ $Å^3$ with 7000 maximum iterations and a spring constant of 1 / $Å^4$, a time step of 0.01 fs and a maximum movement per iteration of 0.05 Å.

3. DFT and Fukui indices for reactive sites determination

3.1. Radical site attack determination on organic acids

Density Functional theory (DFT) provides granular exactness to chemical parameters including; electro negativity, hardness (acidic) and softness (alkalinity) and has associated the parameters with a molecular vibrational approach to chemical reactivity. Most reactions can be classified based on the electrophilic or nucleophilic behaviour of the reactants and products involved and the reactive index (with reference to global softness can be related to intra- and inter-molecular reactivity) when combined with density functional theory can determine the reactive sites for sonochemical degradation.

Chemical potential, chemical hardness and softness and reactivity indices have been used to assess the reactivity of chemical species from their intrinsic electronic properties. In density functional theory, hardness (η) is defined as:

$$= \frac{1}{2}\left(\frac{\delta^2 E}{\delta N^2}\right) v(r) = \frac{1}{2}\left(\frac{\delta \mu}{\delta N}\right)_v \quad (1)$$

where E is the total energy, N is the number of electrons of the chemical species and μ is the chemical potential.

The global softness,S, is defined as the inverse of the global hardness (η).

$$S = \frac{1}{2\eta} = \left(\frac{\delta N}{\delta \mu}\right)_v \quad (2)$$

Arguably, one of the most successful methods is the frontier orbital theory of Fukui [14]. This theory relates the reactivity of a molecule with reference to electrophilic or nucleophilic attack to the charge density arising from the highest occupied molecular orbital (HOMO) or lowest unoccupied molecular orbital (LUMO), respectively. Such DFT-based local properties, e.g., Fukui functions and local softness as reactivity index, were applied for determining electrophilic and nucleophilic reactive species, to allow the identification the attack sites.

3.2. Fukui reactive indices

The Fukui function is defined as the differential change in electron density due to an infinitesimal change in the number of electrons [15]. Parr and Gazquez defined $f(r)$ as [16]:

$$f(r) = \left[\frac{\delta \mu}{\delta v}(r)\right]_N = \left[\frac{\delta \rho(r)}{\delta N}\right]_v \quad (3)$$

The function 'f' is a local quantity, with changing values at different points in the species; N is the total number of electrons; μ is the chemical potential and v is the potential acting on an electron due to all nuclei present. In a finite difference approximation, the condensed Fukui function [14] of an atom, denoted as $\times$, in a molecule with N electrons can be defined as:

$$f_x^+ = [q_x(N+1) - q_x(N)\,] \text{ (for nucleophilic attack)} \quad (4)$$

$$f_x^- = [q_x(N) - q_x(N-1)] \text{ (for electrophilic attack)} \quad (5)$$

$$f_x^0 = \frac{1}{2}[q_x(N+1) - q_x(N-1)\,] = \frac{f_x^+ + f_x^-}{2} \text{ (for radical attack)} \quad (6)$$

where q_x is the electronic population of atom x in a molecule.

In certain anomalous cases, a specific atom shows both a high degree of electrophilicity and nucleophilicity due to the limitation of various basis set dependent charge calculation procedures. Roy *et al.* [17], introduced the concept of *relative* electrophilicity/nucleophilicity to address an anomalous case of predicting intramolecular reactivity of carbonyl compounds and defined relative nucleophilicity as the nucleophilicity of a site relative to its own electrophilicity, and vice versa for electrophilicity.

In accordance with the experimental work of R. Singla [2], the Fukui function was determined for all the major structures in Fig. 1 as well as 3, 4-dihydroxybenzoic acid. Charges were found in ORCA software via the Hirshfeld Population Analysis of the neutral, cationic, and anionic state. The likely reactive sites found supported the degradation schematic reported by R. Singla with the exception of the misidentification as salicylic acid instead of 3-hydroxybenzoic acid and the formation of 2, 3-dihydroxy benzoic acid rather than 3, 4-dihydroxybenzoic acid.

These modifications presented in Part 1 of this study were confirmed by the Fukui calculations and an additional NEB-TS calculation of benzoic acid to phenol by OH radical attacks yielded 3hBA as a transition state [5]. The Fukui coefficients of 3-hydroxybenzoic acid suggested 3, 4-dihydroxybenzoic acid as the product rather than the suggested 2, 3-dihydroxybenzoic acid.

Table 1 summarizes the Fukui radical attack values of 3hBA and Fig. 2 depicts the new suggested site of attack using Avogadro (Fig. 2a) and MultiWfn (Fig. 2b). Fig. 2b is represented with green overlays above atoms with the magnitude of overlays indicating the probability of reactive sites. It should be noted that the atomic numbering system (starting at 0 or 1) is a consequence of software selection and use. In this study and subsequent explanation, we apply the nomenclature based on Avogadro's software. With carbon C5 having the greatest charge density, 3, 4-dihydroxy benzoic acid was pursued computationally as an alternate reaction route.Fig. 3..

3.3. Quantum mechanics – nudged elasticity band analysis of benzoic acid

In quantum mechanics, (QM), sonochemical degradation can be described by the nudged elastic band (NEB) method. This approach can be used to find a minimum energy path (MEP), given only the stable reactant and product state, allowing the determination of the intermediate steps and energy barrier associated with the process. The reaction pathway is built by interpolation of the optimization of a series of intermediate images along the reaction path. The intermediates are bonded together with springs; to always remain constrained between the reaction states. As a result, the reaction states act as an elastic chain. The NEB approach finds a true force that applies to atoms, only the component normal to the reaction path is used, in this case the force due to the springs. The NEB converged when the sum of all forces is zero. The highest energy state is moved along the reaction path to maximize its energy and determine the transition state or at least one saddle-point.

4. Results and discussion

4.1. NEB

Transition states between reactants and products allow the determination of the highest energy. To achieve this state, a multitude of initial state (reactants) to final state (products) must be taken into account and their energy was determined to confirm that the transition state is identified accurately. The NEB approach generates and optimizes many intermediate molecular configurations along the reaction path to find the minimum energy path (MEP). The constructed configurations are systematic linear distributions of the positions between the reactants and products. To achieve reaction path continuity, a spring interaction is included between the adjacent configurations to imitate an elastic band. Spring constants for two molecular configurations are typically fixed, but variable spring constants can also be applied to increase the density of configurations near the top of the energy barrier to further improve estimates of the reaction coordinate near the saddle point [18]. Therefore, the reactant and product position are inputs, and the outputs are position and structure with the highest saddle point, which determines the rate of the elementary reaction. Climbing image NEB with transition state (NEB-TS) method identifies the highest saddle point more accurately [19]. NEB-TS always has one image at the highest saddle point and shows the activation energy precisely with a reduced computational cost. However, NEB methods rely on static molecular configurations. In case of radical-acid reactions occurring in water, the hydrogen bonding network undergoes dynamic changes and a stepwise approach is applied to determine the reaction activation energy barrier [20,21,22,23] and

Table 1
Typical radical attack site determination using Hirshfeld Population Analysis and Fukui Indicators (coefficients) on 3-hydroxybenzoic acid.

Output Label		.xyz File Label	Charges			Fukui Function
Number	Atom		Neutral	Cation	Anion	Radical Attack
7	C	C5	−0.038282	0.092543	−0.098887	0.095715
9	C	C7	−0.038978	0.041531	−0.148066	0.0947985
0	O	O1	−0.197069	−0.051958	−0.239153	0.0935975
5	O	O2	−0.296034	−0.243514	−0.413123	0.0848045
2	C	C2	−0.050628	0.027947	−0.126598	0.0772725
1	C	C1	0.091981	0.188147	0.044706	0.0717205
3	C	C3	−0.014092	0.043656	−0.087884	0.06577
8	C	C6	−0.026326	0.037099	−0.092546	0.0648225
4	C	C4	0.229834	0.243926	0.127303	0.0583115
15	H	H6	0.040741	0.086381	−0.015395	0.050888
14	H	H5	0.039049	0.082911	−0.005368	0.0441395
13	H	H4	0.036985	0.087712	−0.000318	0.044015
6	O	O3	−0.181972	−0.157579	−0.242771	0.042596
11	H	H2	0.037247	0.077864	−0.002423	0.0401435
10	H	H1	0.181864	0.230676	0.156915	0.0368805
12	H	H3	0.183622	0.210408	0.141268	0.03457

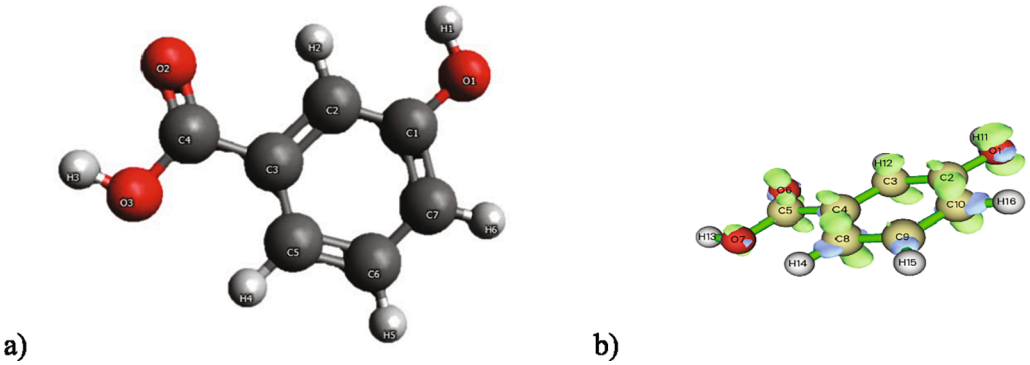

Fig. 2. Representation of 3-hydroxybenzoic acid radical attack sites: 2a) charges from Avogadro 2b) Fukui functions.

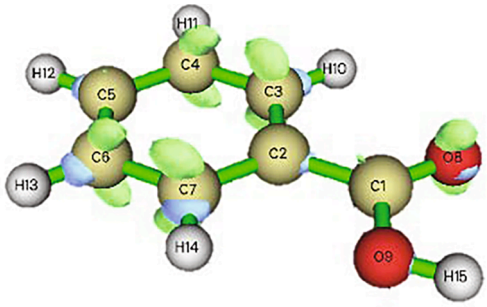

Fig. 3. Benzoic acid with Fukui electron densities represented as green overlays above atoms.

are validated with previously reported results [1].

In order to implement the NEB method, the reactant and product were first geometrically optimized, ensuring no inconsistencies when performing the vibrational frequency analysis. The product states for each stage of the reaction were determined using the modified reaction pathway proposed adapted from R. Singla *et al.* [2] in conjunction with the respective Fukui coefficients. All NEB-TS simulations were also not obtained, specifically on some of the major structures suggested by Singla, namely 3, 5-cyclohexandiene 1, 2-diol and p-benzoquinone. This is supported by R. Singla's findings as under 1% for both the diol and p-benzoquinone were detected after sonolytic degradation of 0.4 mM benzoic acid.

A majority of the studied reaction pathway involved the migration of a •OH to a vacancy created by hydrogen abstraction. This was represented as a crossing of the energy barrier in the obtained MEP. The energy profile for BA sonochemical degradation (Figs. 4 and 5) shows the intermediates of benzoic acid to 3-hydroxybenzoic acid and notes the formation of only one transition state as the saddle point.

The NEB method provided the structures and energies of the various compounds along the reaction pathway. The saddle point configurations, as potential molecular structures, were further confirmed using vibrational frequency analysis as transition state configurations have only one imaginary frequency. This is considered to be general acceptance of transition state due to bond stretching before formation or cleavage. The vibrational frequency analysis also provided the Gibb's reaction energy and was applied to determine the molecular reaction rate constant. This approach could not be applied to the conglomerates or adducts formed in Part 1 as substitute radicals similar to $OH^{\bullet}$ substitution with a water molecule cannot be found in all simulations to maintain the charge and spin state during the reaction step. Nevertheless, the approach allows for the determination of sonochemical degradation compounds as elucidated in Fig. 5.

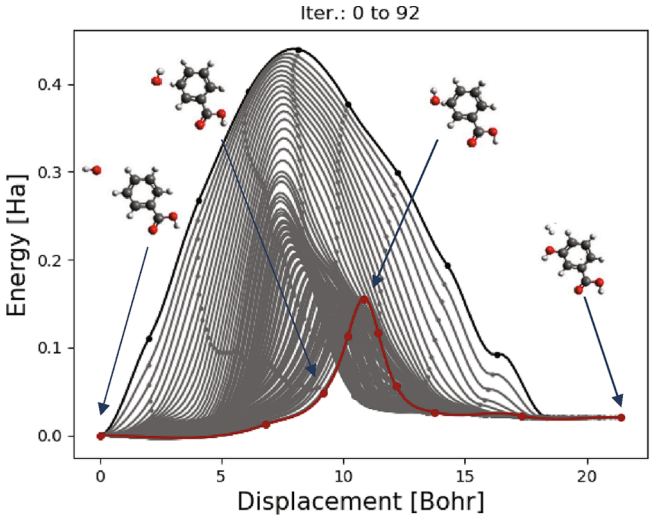

Fig. 4. Minimum Energy Pathway obtained from the Nudged Elastic Band approach for benzoic acid to 3-hydroxybenzoic acid.

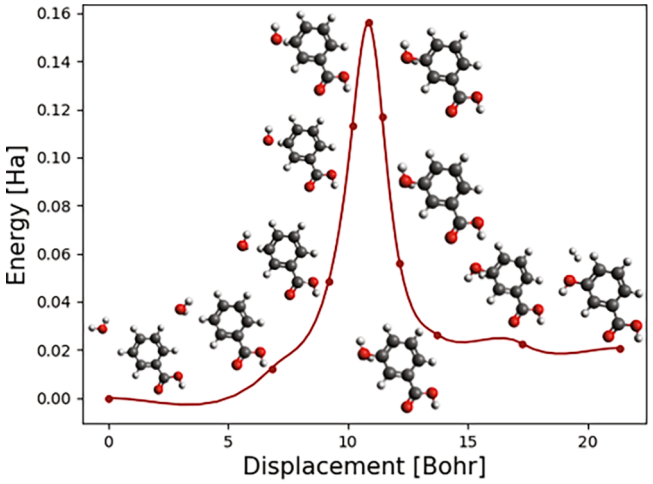

Fig. 5. Minimum Energy Pathway for benzoic acid to 3-hydroxybenzoic acid showing intermediate structures along the path.

4.2. *Determination of rate kinetics*

The rate constant of each reaction and thermodynamic properties can be calculated from the harmonic frequencies calculations of each stage in a reaction with the KiSThelP software, listed in Table 2. The

Table 2
Summarizes the rate constants, activation energy and Gibbs free energy obtained for each reaction.

Reaction	$k_{TST/W}$ (cm^3/mole/s)	A (cm^3/mole/s)	E_a (kJ/mol)	$k_{Arrhenius}$ (cm^3/mole/s)	*Wigner*	ΔG (kJ/mol)
Benzoic Acid to 3-Hydroxy Benzoic Acid	3.10E-86	4.88E-19	383.15	3.39E-86	4.86	454.15
3-Hydroxy Benzoic Acid to 3,4-Dihydroxy Benzoic Acid	2.18E-82	9.99E-18	368.69	2.37E-82	4.68	432.11
3-Hydroxy Benzoic Acid to Phenol	6.68E-82	2.10E-14	384.82	7.41E-82	1.00	425.51
Phenol to Catechol	8.16E-87	4.97E-19	386.50	8.93E-87	4.69	457.36
Phenol to Pyrogallol	1.64E-98	1.51E-18	455.91	1.85E-98	1.01	520.3
Catechol to Pyrogallol	2.84E-86	8.81E-19	384.82	3.12E-86	4.71	454.28
Catechol to Muconic Acid via Oxygen	5.66E-36	4.57E-15	119.18	5.88E-36	1.00	163.48

Arrhenius equation parameters $k_{Arrhenius} = Ae^{\frac{-E_a}{RT}}$ parameters were computed via statistical fitting in the temperature range of 298 K +/- 20%. As the NEB-TS method produces an MEP that yields one saddle point, a bimolecular reaction rate constant can be yielded via Classical Transition State Theory with Wigner Tunneling Correction based on the following equation:

$$k^{TST} = \sigma \frac{k_b T}{h} \left(\frac{RT}{P^0}\right)^{\Delta n} e^{\left(-\Delta G^{\ddagger,0}(T)/k_b T\right)} \tag{7}$$

where k_b is Boltzmann's constant, R is the ideal gas constant, T is the temperature, h is Planck's constant. $\Delta G^{\ddagger,0}(T)$ represents the standard Gibbs free energy of activation for the considered reaction ($\Delta n = 1$ or 0 for gas-phase bimolecular or unimolecular reactions, respectively; RT/P^0 has the unit of the inverse of concentration) [24].

In the calculation of $\Delta G\ddagger,0(T)$, the imaginary frequency that corresponds to the reaction coordinate degree of freedom is incorporated by a multiplicative transmission coefficient $\chi(T)$ used to compute the Wigner tunneling correction [25] as noted in the following equations:

$$Wigner = \chi(T) = 1 + \frac{1}{24}\left(\frac{hIm(v^{\ddagger})}{k_b T}\right)^2 \tag{8}$$

$$k^{TST/W} = \chi(T) \times k^{TST} \tag{9}$$

The experimental kinetic energy data is summarised in Table 2 based on experimental and calculated results for the addition of ·OH to the hydroxylated and decarboxylated benzene compounds.

4.3. Implementation of linear free energy relationships

Linear free energy relationship rate constant k_{LFER} is based on earlier work [26] which determined the following equation for organic compounds.

$$\ln k_{chem} = -0.19\Delta G^{act}_{aq,calc} + 21.09 (n = 14) \tag{10}$$

Aqueous phase advanced oxidation processes (AOPs) under ultrasound produce •OH radicals oxidize electron rich organic compounds. Accordingly, there is a need to develop a first-principles kinetic model that can predict the dominant reaction pathways that explain the degradation of products. Earlier published work [26,27] have reported LFERs that relate experimentally obtained kinetic rate constants to aqueous phase free energies of activation determined by quantum mechanics.

Similar to the earlier published data, a new LFER was established from Table 2:

$$\ln\left(k_{TST/W}\right) = -1.677\Delta G - 15.41 \tag{11}$$

With an R^2 value of 0.9997 derived from Fig. 6.

4.4. Additional calculations – Mulliken charges, polarizability, dipole moments, HOMO-LUMO energy gap

Upon NEBT-TS saddle point determination, interaction energies, Mulliken charges, dipole moment, polarizability, and frontier orbitals were calculated for each stage in the minimum energy pathway to confirm the validity of the reaction intermediates. The theoretical determination of charge properties and the energy band gap were compared to similar studies by S. Riahi's group for similar naphthenic acids [1]. Although, Riahi's *et* al. examined the properties in terms of adsorption, similar trends are shown in sonochemical product formation of radical attack reactions and their transition states.

Mulliken charges, determined through Mulliken population analysis, were applied to characterize the electronic charge distribution in a molecule and thus can be used to evaluate the bonding or non-bonding nature between pairs of atoms. The charges are determined in all single point calculations or at the beginning and end of all geometric optimizations in quantum chemistry application software such as ORCA and Gaussian 09. It is noteworthy that Mulliken charges are sensitive to the basis set selection and can be ill-defined [19]. The application of Mulliken charges as physical measures for bond evaluation is poor due to the lack of physical limitations as the basis set converges. Hirshfeld Population Analysis and Fukui indexes are by far a more accurate representation of charge density. Despite this, it is not invaluable to review the charges as they roughly reflect what one could expect from atoms based on their electronegativity [28].

Similar to the findings from Riahi's study, there is no significance in terms of charge transfer between the atoms before and after the attack. Notably, the Mulliken charges identify that the carbon at the site of radical attack typically has the greatest Mulliken charge followed by the hydrogen connected to it as shown in Fig. 7. The most negative charges are the oxygen atoms on the naphthenic acid or radicals due to highest electronegativity. As such, the expected interaction is between the radical oxygen with a carbon site on the naphthenic acid's aromatic ring one would predict via organics. This general trend can be seen in all benzoic acid degradation products with discrepancies corresponding to their respective functional group substitutions. Combining Mulliken charges with Fukui indexes, the most probable radical attack site can be identified among the possible sites of attack in the ring structure.

The dipole moment is the first derivative of energy with respect to an applied electric field and thus is a measure of asymmetry depending on their molecular charge distribution. Similarly, polarizability is the ease for which the electron clouds of a symmetric neutral species distort with respect to the electric field. From Riahi's work, it is noted that the adsorbed structure had the highest dipole moment and polarizability values across their structures consistent with their adsorption energies. Similarly, as shown for sonochemical reactions, the transitions state of a radical attack has greater dipole moment in the MEP due to the asymmetry of the newly added OH group as depicted in Table 3. The polarizability showed a similar trend however it was not as definitive as the dipole moments as non-transition state images in the MEP were found to show higher polarizability. The changes in dipole moment and

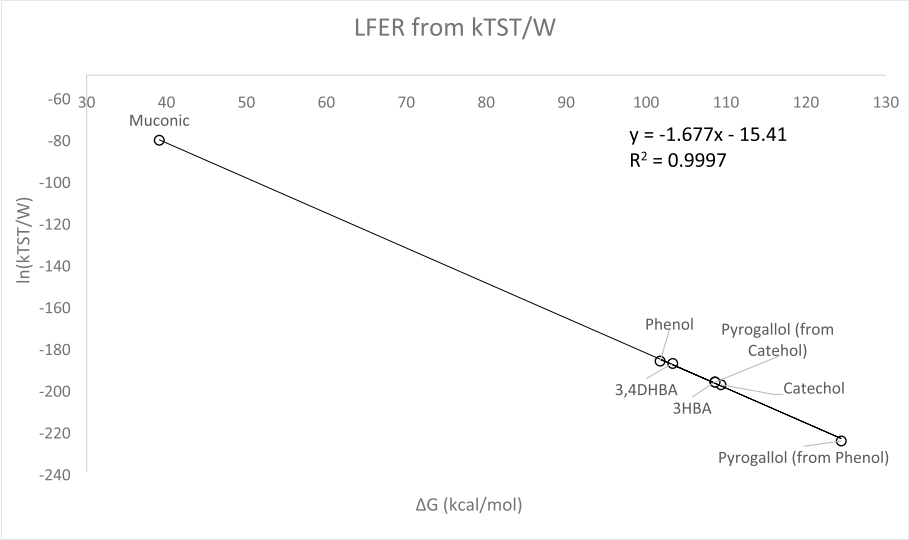

Fig. 6. Plot of LFER obtained from each intermediate using k_{TST}.

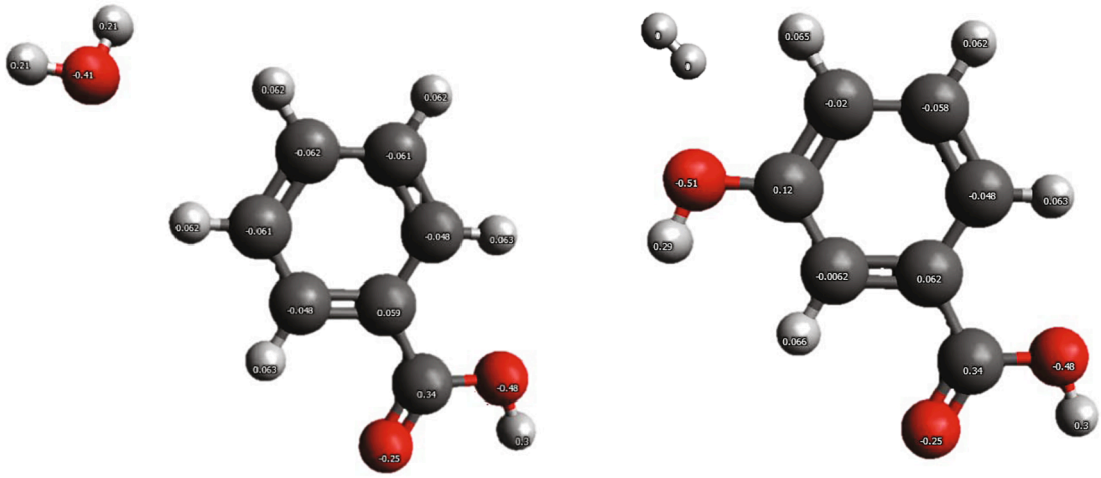

Fig. 7. Mulliken charges of benzoic acid before (left) and after (right) radical attack by water.

Table 3
Electronic properties of benzoic acid degradation products' transition states.

Reaction	Dipole Moment (Debye)	Polarizability (Å^3)
Benzoic Acid to 3-Hydroxy Benzoic Acid	3.05947	97.99688
3-Hydroxy Benzoic Acid to 3,4-Dihydroxy Benzoic Acid	2.72303	106.4105
3-Hydroxy Benzoic Acid to Phenol	5.23937	100.2082
Phenol to Catechol	2.55821	83.26008
Phenol to Pyrogallol	2.46185	89.86154
Catechol to Pyrogallol	2.46127	86.84641
Catechol to Muconic Acid via Oxygen	3.5195	95.20215
Catechol to Muconic Acid via H2O2	5.61836	99.95786

Table 4
Frontier orbital data of benzoic acid degradation products in electron volts.

Reaction	HOMO (eV)	LUMO (eV)	Energy Band Gap (eV)
Benzoic Acid to 3-Hydroxy Benzoic Acid	−5.4737	−1.301	4.1727
3-Hydroxy Benzoic Acid to 3,4-Dihydroxy Benzoic Acid	−6.4585	−2.9177	3.5408
3-Hydroxy Benzoic Acid to Phenol	−5.2803	−1.2389	4.0414
Phenol to Catechol	−4.8342	−0.3507	4.4835
Phenol to Pyrogallol	−4.8318	−0.2650	4.5668
Catechol to Pyrogallol	−4.8146	−0.2630	4.5516
Catechol to Muconic Acid via Oxygen	−5.5729	−3.5279	2.0450
Catechol to Muconic Acid via H2O2	−5.7082	−3.0088	2.6994

polarizability throughout the MEP again reflects the interaction of an ultrasound generated radical successfully attacking the acid.

Evaluating the frontier orbital energies to find HOMO (Highest Occupied Molecular Orbital) and LUMO (Lowest Occupied Molecular Orbital) energies for each reaction step yields an expected result where the energy gap ($E_{LUMO} - E_{HOMO}$) of the stage identified as the transition state in the MEP was the lowest among all the transition images as shown in in Table 4.Typically applied in photochemical reactions and extended to evaluate semiconductor potential in solids, the small close energy gap of the frontier orbitals can be reviewed as a stability analysis of aromatic compounds due to conjugated pi systems. Thus, akin to Riahi's absorbed species, the low energy gap highlights the transition state found by NEB-TS is indeed the most stable stage within the reaction.

5. Conclusions

In summation, density functional theory calculations have been used to study the sonochemical degradation pathways of benzoic acid in aqueous solutions to identify and explore the full mineralization pathways. Nudge Elastic Band Transitions State method in ORCA 4.2 was used to explore the validity of reaction profiles computationally. In conjunction with this approach, Fukui indices were calculated from Hirshfeld population values to determine exact sites of radical attack, in which the data supports a more linear pathway for benzoic acid degradation adapted from the scheme postulated by R. Singla *et al.* [2]. The use of NEB method identified molecular intermediate structures accurately during fragmentation. A linear free energy relationship of the computational benzoic acid degradation was established with classic transition state theory alongside Wigner Tunneling to be $\ln(k_{TST/W}) = -1.677\Delta G - 15.41$ with a R^2 of 0.9997. By means of the developed approach, multiple properties such as dipole moments, polarizability, Mulliken charges, Hirshfeld population values, and energies of the frontier molecular orbital were also inferred. The results of these properties were compared to the literature values of earlier computational work [1] to validate the calculated transition state by NEB-TS. These findings will allow further exploration and understanding of fragmentations and eventual mineralization of NA compounds. This two part study sets a methodological baseline for extensive exploration of naphthenic acid remediation in OSPW using sonochemical methods.

Funding

This work was supported by Canadian federal government; Organization of Energy Research and Development funding program (OERD No: NRC-19–115) and NRC's Environmental Advances in Mining (EAM) program.

Author contribution

All authors have given approval to the final version of the manuscript.

CRediT authorship contribution statement

Deepak M. Kirpalani: Conceptualization, Investigation, Data curation, Methodology, Software, Writing – original, reviewing and editing, Funding acquisition. **Andy Nong:** Investigation, Data curation, Formal Analysis, Writing – original draft. **Rija Ansari:** Writing – Investigation, Formal analysis, Validation, Writing – Original draft, reviewing and editing.

Declaration of Competing Interest

The authors declare that they have no known competing financial interests or personal relationships that could have appeared to influence the work reported in this paper.

Acknowledgement

The authors acknowledge the support from the Environmental Advances in Mining Program at the National Research Council of Canada.

References

[1] S. Riahi, P. Pourhossein, M.R. Ganjali, Removal of naphthenic acids from liquid petroleum: theoretical study, Pet. Sci. Technol. 28 (1) (2010) 68–78.
[2] R. Singla, M. Ashokkumar, F. Grieser, The mechanism of the sonochemical degradation of benzoic acid in aqueous solutions, Res. Chem. Intermed. 30 (7) (2004) 723–733.
[3] R.J. Johnson, B.E. Smith, P.A. Sutton, T.J. McGenity, S.J. Rowland, C. Whitby, Microbial biodegradation of aromatic alkanoic naphthenic acids is affected by the degree of alkyl side chain branching, ISME J. 5 (3) (2011) 486–496.
[4] C. Wu, A.D. Visscher, I.D. Gates, On naphthenic acids removal from crude oil and oil sands process-affected water, Fuel 253 (2019) 1229–1246.
[5] R. Ansari, D.M. Kirpalani, Insights into ultrasound-promoted degradation of naphthenic acid compounds in oilsands process affected water, Ultrason. Sonochem. 83 (2022) 105929.
[6] C.v. Sonntag, P. Dowideit, F. Xingwang, R. Mertens, P. Xianming, M. N. Schuchmann, et al., The fate of peroxyl radicals in aqueous solution, Water Sci. Technol. 35 (4) (1997) 9–15.
[7] P. Krystynik, Advanced Oxidation Processes (AOPs) – Utilization of Hydroxyl Radical and Singlet Oxygen. 2021.
[8] A.D. Becke, Density-functional thermochemistry. III. The role of exact exchange, J. Chem. Phys. 98 (7) (1993) 5648–5652.
[9] C. Lee, W. Yang, R.G. Parr, Development of the Colle-Salvetti correlation-energy formula into a functional of the electron density, Phys. Rev. B 37 (2) (1988) 785–789.
[10] S.H. Vosko, L. Wilk, M. Nusair, Accurate spin-dependent electron liquid correlation energies for local spin density calculations: a critical analysis, Can. J. Phys. 58 (8) (1980) 1200–1211.
[11] T.A. Halgren, Merck molecular force field. I. Basis, form, scope, parameterization, and performance of MMFF94, J. Comput. Chem. 17 (5-6) (1996) 490–519.
[12] D.W. Schwenke, D.G. Truhlar, Systematic study of basis set superposition errors in the calculated interaction energy of two HF molecules, J. Chem. Phys. 82 (5) (1985) 2418–2426.
[13] U. Frisch, B. Hasslacher, Y. Pomeau, Lattice-gas automata for the Navier-Stokes equation, Phys. Rev. Lett. 56 (14) (1986) 1505–1508.
[14] R.G. Parr, W. Yang, Density functional approach to the frontier-electron theory of chemical reactivity, J. Am. Chem. Soc. 106 (14) (1984) 4049–4050.
[15] P.K. Chattaraj, Chemical Reactivity Theory : A Density Functional View; 2009.
[16] R.G. Parr, J.L. Gazquez, Hardness functional, J. Phys. Chem. 97 (16) (1993) 3939–3940.
[17] S. Pratihar, S. Roy, Nucleophilicity and site selectivity of commonly used arenes and heteroarenes, J. Org. Chem. 75 (15) (2010) 4957–4963.
[18] H. Al-Mahayni, X. Wang, J. Harvey, G.S. Patience, A. Seifitokaldani, Experimental methods in chemical engineering: Density functional theory, Can. J. Chem. Eng. 99 (9) (2021) 1885–1911.
[19] F. Neese, F. Wennmohs, Orca – An ab initio, DFT and semiempirical SCF-MO package. 42nd ed. Ruhr, Germany: Max Planck Institut.
[20] T.K. Woo, P.M. Margl, T. Ziegler, P.E. Blöchl, Static and ab initio molecular dynamics study of the titanium(IV)-constrained geometry catalyst (CpSiH2NH)Ti-R +. 2. Chain termination and long chain branching, Organometallics 16 (15) (1997) 3454–3468.
[21] C. Jarzynski, Nonequilibrium equality for free energy differences, Phys. Rev. Lett. 78 (14) (1997) 2690–2693.
[22] H. Oberhofer, C. Dellago, P.L. Geissler, Biased sampling of nonequilibrium trajectories: can fast switching simulations outperform conventional free energy calculation methods? J. Phys. Chem. B 109 (14) (2005) 6902–6915.
[23] X. Zhao, Y. Liu, Unveiling the active structure of single nickel atom catalysis: critical roles of charge capacity and hydrogen bonding, J. Am. Chem. Soc. 142 (12) (2020) 5773–5777.
[24] KiSThelP 2021 User Documentation III.3 Description of the Calculation Menu. [Online]; 2021. Available from: http://kisthelp.univ-reims.fr/userDocumentation/calculationMenu.html.
[25] H. Pelzer, E.P. Wigner, Über die Geschwindigkeitskonstante von Austauschreaktionen, Z. Phys. Chem. 1 (1932) 69–95.
[26] D. Minakata, W. Song, S.P. Mezyk, W.J. Cooper, Experimental and theoretical studies on aqueous-phase reactivity of hydroxyl radicals with multiple carboxylated and hydroxylated benzene compounds, PCCP 17 (17) (2015) 11796–11812.
[27] D. Minakata, S.P. Mezyk, J.W. Jones, B.R. Daws, J.C. Crittenden, Development of linear free energy relationships for aqueous phase radical-involved chemical reactions, Environ. Sci. Technol. 48 (23) (2014) 13925–13932.
[28] A. Tomberg, GAUSSIAN 09W TUTORIAL: McGill University; 2012.